

$\pi\eta$  PHOTOPRODUCTION ON THE NUCLEON\*

ŁUKASZ BIBRZYCKI

Chair of Computer Science and Computational Methods  
Pedagogical University of Cracow  
Podchorążych 2, 30-084 Kraków, Poland

ROBERT KAMIŃSKI

The Henryk Niewodniczański Institute of Nuclear Physics  
Polish Academy of Sciences  
Radzikowskiego 152, 31-342 Kraków, Poland

*(Received May 25, 2015)*

We calculate the amplitude of the  $\pi\eta$  photoproduction on the proton and the associated cross sections. The primary objective of the model is to describe the photoproduction of the isovector resonances in the  $\pi\eta$  channel which is important in the context of elucidating the nature of the scalar  $a_0(980)$  meson. The model can be also applied to description of the photoproduction of tensor isovector resonance  $a_2(1320)$ .

DOI:10.5506/APhysPolBSupp.8.419

PACS numbers: 14.40.Be, 13.60.Le, 12.39.Mk

## 1. Introduction

Proper description of the light meson spectrum is the key to understanding the nonperturbative sector of the QCD. In spite of a few decades of both theoretical and experimental effort, the hadron spectroscopy is still full of open questions. For the scalar–isoscalar nonet, even its composition is a subject of the debate [1]. There is, however, the common belief that at least some scalar resonances are not standard  $q\bar{q}$  states but rather tetraquark  $qq\bar{q}\bar{q}$  or molecular systems. In particular, it was shown [2] that the  $\phi(1020) \rightarrow f_0(980)\gamma$  and  $\phi(1020) \rightarrow a_0(980)\gamma$  decays are dominated by the kaon-loop transition, which supports the molecular picture of the scalar resonances  $f_0(980)$  and  $a_0(980)$ . The lightest scalar–isoscalar resonance  $f_0(500)$  whose very existence was disputed in the past has been firmly established

---

\* Presented at “Excited QCD 2015”, Tatranská Lomnica, Slovakia, March 8–14, 2015.

and its mass and width precisely determined [3]. There is a mounting evidence, however, that  $f_0(500)$  (formerly known as  $\sigma$ ) has a non- $q\bar{q}$  nature which is manifested by its strongly nonlinear Regge trajectory [4]. On the other hand, the vector and tensor mesons seem to fit well to standard  $q\bar{q}$  nonets. Therefore, the successful attempts to describe tensor mesons as dynamical systems created due to final state  $\pi\pi$  [5], and  $\rho\rho$  [6] interactions are quite surprising. Related to the problem of the resonances' internal structure is the question of their production and decay mechanisms. In this respect, the mechanisms of the radiative decays and photoproduction are of special importance since they are believed to bring important information on the meson internal structure. In this work, we focus on the photoproduction of scalar isovector resonances in the  $\pi\eta$  channel with a special emphasis on the  $a_0(980)$  resonance. We also speculate on the consequences of our model for the photoproduction of the  $\pi\eta$  pairs in the higher partial waves.

## 2. Model description

In our model, the resonance is photoproduced through the two-stage process. In the first stage, a  $\pi\eta$  pair is photoproduced. This stage is described in terms of the Born amplitudes whose diagrammatic representation is shown in Fig. 1. In principle, one could also include in the model the diagrams with the pseudoscalar exchanges but in the energy region of our

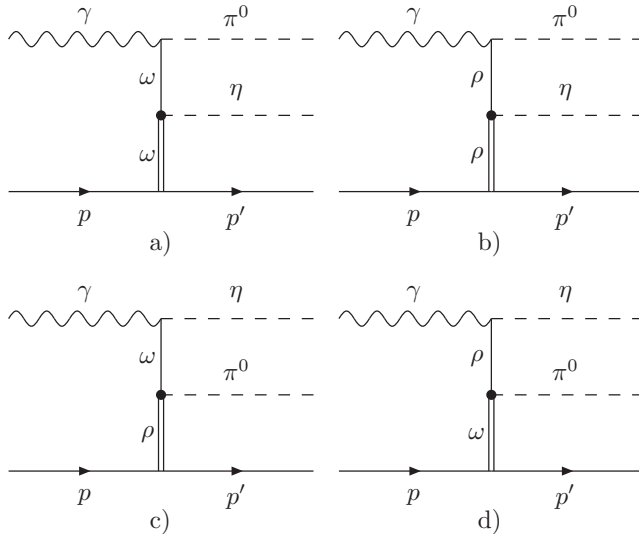


Fig. 1. Diagrammatic representation of the Born amplitudes of the  $\pi\eta$  photoproduction on the proton.

interest *i.e.* photon beam energy at upgraded JLab facility, these exchanges seem negligible. In this introductory study, we neglect the effects of the interchannel coupling *i.e.* we do not take into account the Born amplitudes of the  $K^+K^-$  and  $K^0\bar{K}^0$  photoproduction. This is justified by the fact that in the coupled channel analyses of the  $\pi\eta$ - $K\bar{K}$  system performed so far, the obtained inter channel coupling was indeed small [7].

In the second stage, the  $\pi\eta$  pair undergoes the final state re-scattering which may result in the resonance creation [7]. Thus the complete photoproduction amplitude can be schematically depicted as in Fig. 2. Analogous approach was successfully applied to the  $f_0(980)$  photoproduction in the  $K\bar{K}$  [8] and  $\pi^+\pi^-$  [9] channels as well as to the description of the resonant  $\pi\pi$  photoproduction in the  $D$ -wave [5].

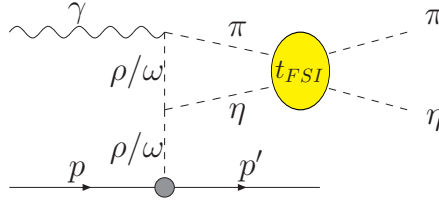


Fig. 2. Diagrammatic representation of the resonance photoproduction through the final state interactions.

The complete photoproduction amplitude, *i.e.* including the  $\pi\eta$  final state interactions, projected on the  $L^{\text{th}}$  partial wave, reads

$$\begin{aligned} \langle \lambda' M | A_{\pi\eta}^L | \lambda_\gamma \lambda \rangle &= \langle \lambda' M | \hat{V}_{\pi\eta}^L | \lambda_\gamma \lambda \rangle \\ &+ 4\pi \int_0^\infty \frac{k'^2 dk'}{(2\pi)^3} F(k, k') \hat{t}_{\pi\eta}^L G_{\pi\eta}(k') \langle \lambda' M | \hat{V}_{\pi\eta}^L | \lambda_\gamma \lambda \rangle, \end{aligned} \quad (1)$$

where  $\hat{V}_{\pi\eta}^L$  is the Born amplitude of the  $\pi\eta$  photoproduction,  $\hat{t}_{\pi\eta}^L$  is the  $\pi\eta$  elastic scattering amplitude,  $\lambda, \lambda', \lambda_\gamma$  and  $M$  are, respectively, the helicities of the initial and final proton, photon helicity and projection of the  $\pi\eta$  system angular momentum on the spin quantisation axis  $z$  (thus 0 for the  $S$ -wave).  $\hat{G}$  is the propagator of the intermediate  $\pi\eta$  pair and  $F(k, k')$  is the form-factor needed to regularize divergent mesonic loop of the diagram shown in Fig. 2. Current analysis is limited to the on-shell part of the amplitude defined by Eq. (1), so after the momentum integration, it can be recast as

$$\langle \lambda' M | A_{\pi\eta}^L | \lambda_\gamma \lambda \rangle = [1 + ir_{\pi\eta} \hat{t}_{\pi\eta}^L] \langle \lambda' M | V_{\pi\eta}^L | \lambda_\gamma \lambda \rangle, \quad (2)$$

where  $r_{\pi\eta}$  is the kinematical factor and reads  $r_{\pi\eta} = -|k|M_{\pi\eta}/8\pi$  and  $|k|$  is the modulus of the momentum in the  $\pi\eta$  center-of-mass system. This

limitation may be important as it was shown in [10] that the off-shell part of the amplitude is both significant and strongly dependent on the cut-off parameter but fortunately its impact on the amplitude is close to the overall re-scaling. Equation (2) shows that the spin structure of the photoproduction amplitude for the resonances decaying to two pseudoscalars is entirely determined by the Born amplitude.

### 3. Results

With the partial wave photoproduction amplitude defined in Eq. (2), we define the double differential cross section as

$$\frac{d\sigma^L}{dt dM_{\pi\eta}} = \frac{1}{4} \frac{1}{(2\pi)^3} \frac{|k|}{32m^2 E_\gamma^2} \sum_{\lambda_\gamma, \lambda, M, \lambda'} |\langle \lambda' M | A_{\pi\eta}^L | \lambda_\gamma \lambda \rangle|^2, \quad (3)$$

where  $m$  and  $E_\gamma$  are the proton mass and photon energy in the laboratory frame respectively. The  $S$ -wave mass distribution for both the Born and complete photoproduction amplitudes obtained after  $t$ -integration of Eq. (3) is shown in Fig. 3. The distribution we have obtained exhibits the large and

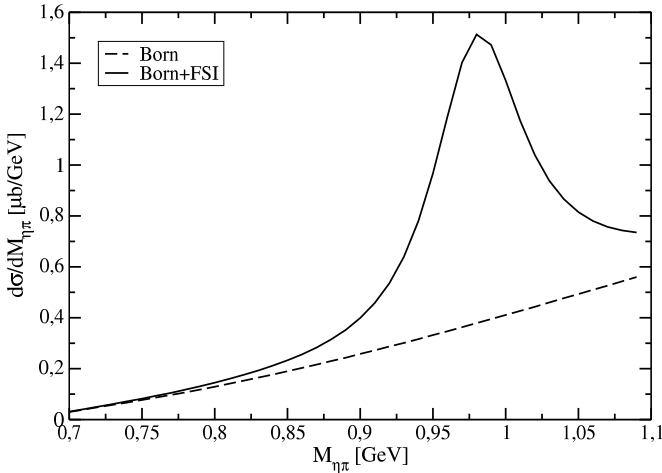


Fig. 3.  $S$ -wave mass distribution  $d\sigma/dM_{\pi\eta}$  at photon energy  $E_\gamma = 5$  GeV.

rising Born background which is qualitatively in line with the high energy bins of the mass distributions obtained by the CBELSA/TAPS Collaboration [11]. In Fig. 4, we show the differential cross section obtained after integration of Eq. (3) in the  $M_{\pi\eta}$  effective mass region corresponding to the  $a_0(980)$  for both the normal and Regge propagators. Our model is better suited for the photoproduction at higher photon energies ( $\gtrsim 5$  GeV) which

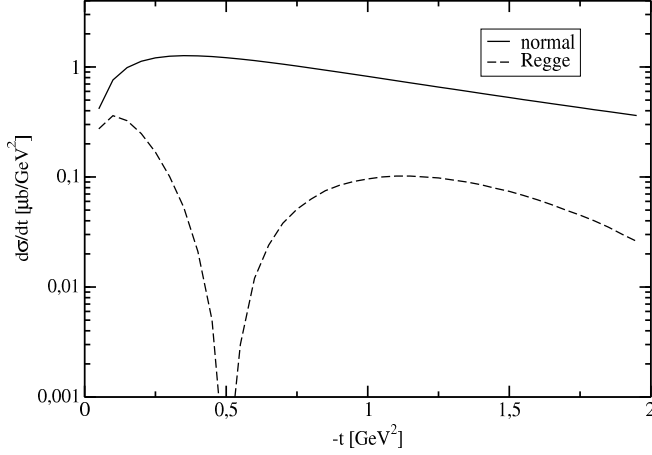


Fig. 4.  $S$ -wave differential cross section  $d\sigma/dt$  at photon energy  $E_\gamma = 5$  GeV.

favours the reggeised amplitude. This suggests, however, that other contributions to the amplitude are necessary to “fill” the minimum observed in the cross section. Apart from the calculations for the  $S$ -wave, we also calculated the double differential cross sections for the  $P$ - and  $D$ -waves along with the cross section for the full amplitude. Figure 5 shows that the cross section is saturated by three lowest partial waves and that the  $S$ -wave dominates. Moreover, the  $P$ -wave is strongly suppressed in comparison to the dominating  $S$ -wave (and  $D$ -wave). This may be crucial for searches of exotic spin 1 mesons (like  $\pi_1(1400)$ ) in photoproduction reactions.

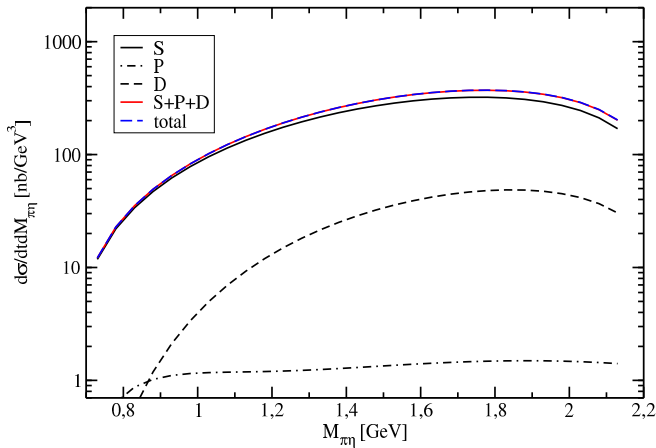


Fig. 5. Double differential cross section  $d\sigma/dtdM_{\pi\eta}$  for the partial waves  $S$ ,  $P$  and  $D$  at photon energy  $E_\gamma = 5$  GeV and  $t = -0.7$  GeV<sup>2</sup>.

#### 4. Conclusions and outlook

We presented the introductory results on the model which describes the isovector resonance photoproduction as a final state interaction effect. We note that the shape of the resonance line and large background are in line with CBELSA/TAPS measurements for largest energies accessible in this experiment. The quantitative conclusions are yet premature since the currently accessible experimental data on the  $\pi\eta$  photoproduction are collected at low energies. Our present calculations do not take into account the off-shell contributions which may be significant. Moreover, the reggeised photoproduction amplitude which seems appropriate for higher photon energies (like those in the upgraded CLAS experiment) requires additional contributions in order to “fill” the minimum which is observed in the model cross section.

Research has been funded by the Polish National Science Center (NCN) grant No. DEC-2013/09/B/ST2/04382.

#### REFERENCES

- [1] K.A. Olive *et al.* [Particle Data Group], *Chin. Phys. C* **38**, 090001 (2014).
- [2] Yu. Kalashnikova *et al.*, *Phys. Rev. C* **73**, 045203 (2006).
- [3] R. Garcia-Martin *et al.*, *Phys. Rev. D* **83**, 074004 (2011).
- [4] J.T. Londergan, J. Nebreda, J.R. Pelaez, A. Szczepaniak, *Phys. Lett. B* **729**, 9 (2014).
- [5] Ł. Bibrzycki, R. Kamiński, *Phys. Rev. D* **87**, 114010 (2013).
- [6] J.J. Xie, E. Oset, [arXiv:1412.3234 \[nucl-th\]](#).
- [7] A. Furman, L. Leśniak, *Phys. Lett. B* **538**, 266 (2002).
- [8] Ł. Bibrzycki, L. Leśniak, A.P. Szczepaniak, *Eur. Phys. J. C* **34**, 335 (2004).
- [9] Ł. Bibrzycki, L. Leśniak, *EPJ Web Conf.* **37**, 09009 (2012).
- [10] C.-R. Ji *et al.*, *Phys. Rev. C* **58**, 1205 (1998).
- [11] E. Gutz *et al.* [CBELSA/TAPS Collaboration], *Eur. Phys. J. A* **50**, 74 (2014).